



Enhanced theoretical models and numerical methods for hypersonic flows

Giuseppe Pascazio

Dipartimento di Meccanica Matematica e
Management, Politecnico di Bari

3rd International Symposium on Hypersonic Flight

Air Force Academy (Pozzuoli), Italy, May 30-31, 2019

AAA – Sez. Roma Due “Luigi Broglio”



Collaborations



FRANCESCO BONELLI
DARIO DE MARINIS



GIANPIERO COLONNA



LUIGI CUTRONE

Liceo Scientifico Statale "Leonardo da Vinci"
Bisceglie Italy

MICHELE TUTTAFESTA

Objective and Outline

Objective:

Development of a High Performance Computing (HPC) CFD code for investigating high enthalpy flows

Outline:

- **Governing equations and numerical method**
- **Thermochemical non-equilibrium models**
- **multi-GPU code performance**
- **Immersed boundary approach**
- **Results**
- **Conclusions**

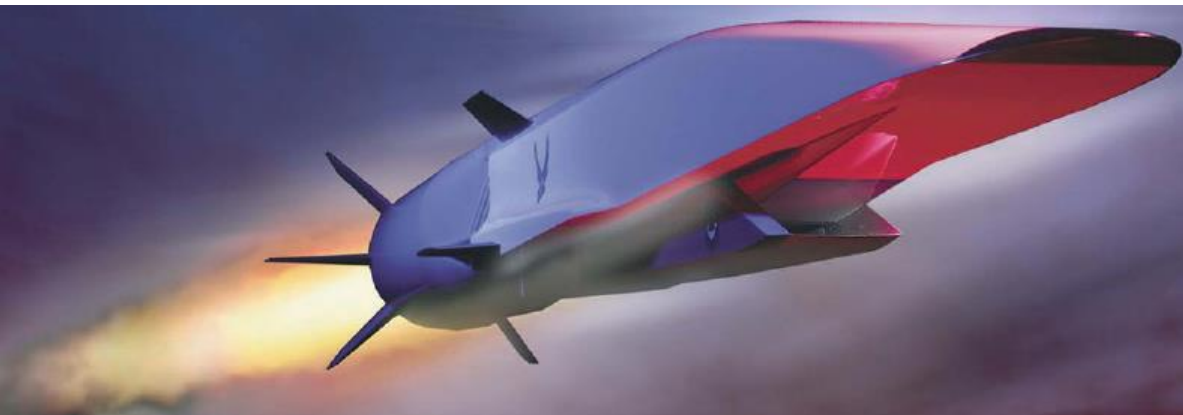
Hypersonic Flight



LAPCAT-A2: outcome of LAPCAT I project for civil Mach 5 transport (courtesy REL)



Transcontinental civil flights: LAPCAT, FAST20xx (source: esa website)



Hypersonic cruise missiles (source: defence Advanced Research Agency illustration)



Orion capsule (source: NASA)

Numerical method

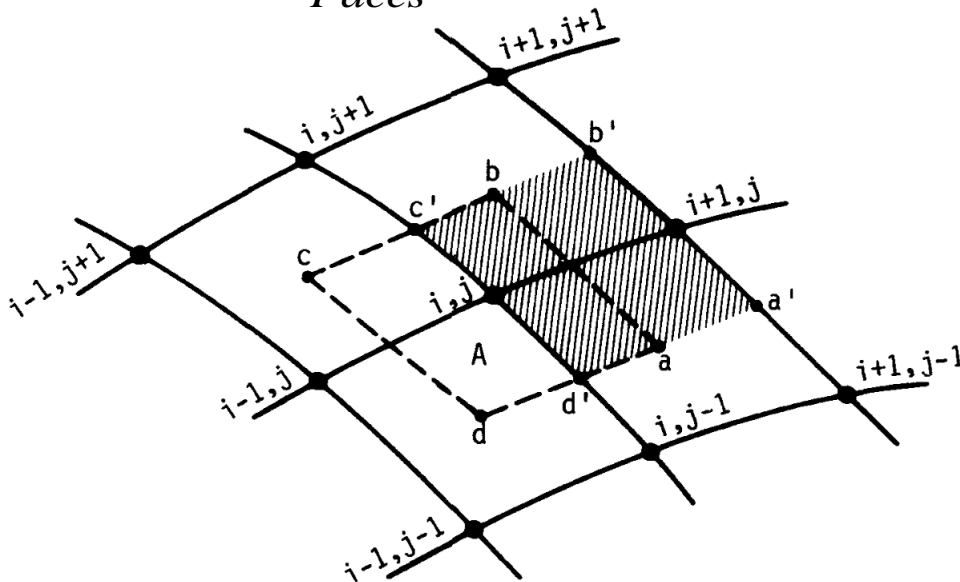
$$V_{i,j} \frac{d\mathbf{U}_{i,j}}{dt} + \sum_{\text{Faces}} \mathbf{F}_{num} \cdot \mathbf{n} \Delta S = V_{i,j} \mathbf{W}_{i,j}$$

*Cell-centered Finite Volume
Space discretization on a
Multi-block structured mesh*

$$\mathbf{F}_{num} = \mathbf{F}_{E,num} - \mathbf{F}_{V,num}$$

Reactive Navier-Stokes equations:

- Advection and pressure term (hyperbolic)
- Shear-stress, heat flux terms (diffusive)
- Chemical source terms (stiffness)



Solution strategy:

➤ **Operator splitting approach: Frozen step + Chemical step**

✓ **Frozen step: Method of Lines:**

• **Space discretization + Time integration**

- **Space discretization: Inviscid & Viscous terms scheme**
- **Time integration: Runge-Kutta scheme**

✓ **Chemical step: implicit scheme for stiff terms**

Operator splitting approach

$$V_{i,j} \frac{d\mathbf{U}_{i,j}}{dt} + \sum_{\text{Faces}} \mathbf{F}_{num} \cdot \mathbf{n} \Delta S = 0$$

Frozen step: AUSM or Flux Vector Splitting of Steger and Warming with MUSCL approach for higher order accuracy; Gauss divergence approach for viscous terms; Runge-Kutta scheme up to third order for time integration

$$\frac{\partial}{\partial t} \int_{V_0} \mathbf{U} dV = \int_{V_0} \mathbf{W} dV$$

Chemical step

$$\Delta t_c^{(v)} = \Delta t_f / n$$

Sub-time step

$$\frac{\partial \mathbf{y}}{\partial t} = \mathbf{P} - \mathbf{L}\mathbf{y} \quad \mathbf{y} = \{\rho_i\}_{0 \leq i \leq N}$$

P is a vector and L a diagonal matrix.

P_i and $L_i y_i$ are non-negative and represent, respectively, production and loss terms for component y_i

$$y_i^k(t + \Delta t_c^{(v)}) = \frac{\Delta t_c^{(v)} P_i(\mathbf{y}^{k-1}) + y_i(t)}{1 + \Delta t_c^{(v)} L(\mathbf{y}^{k-1})}$$

Gauss-Seidel iterative scheme

Thermochemical non-equilibrium models for air

MULTI-TEMPERATURE 5 SPECIES PARK MODEL¹

- 17 reactions + 3 transport equations for the vibrational energies
- Arrhenius type rate coefficients function of an effective temperature calculated as a geometrical mean of translational and vibrational temperatures
- Vibrational levels follow a Boltzmann distribution at temperature T_v
- Tuned on experimental measures
- Not computationally demanding
- It may fail when the conditions are far from those for which it was tuned

5 SPECIES State-to-State (StS) MODEL²

- Detailed vibrational kinetics of molecules.
- 68 and 47 vibrational levels for N_2 and O_2 respectively
- Thousands of elementary processes → High accuracy but huge computational cost

¹ C. Park, Nonequilibrium Hypersonic Aerothermodynamics, Wiley, New York, 1990

² M. Capitelli et al., Fundamentals Aspects of Plasma Chemical Physics: Kinetics, Springer Science & Business Media, 2015

Combined GPU and MPI Computing

GPUs are very powerful and efficient

MPI allow to efficiently scale the computations across a multiple-nodes GPU cluster

**Our implementation has shown
speed-ups (single GPU vs single-core CPU) up to 150**

MPI-CUDA: GPU vs CPU computational performance

NVIDIA Tesla K40 (235 W) VS Intel Xeon CPU E5-2630 (6 cores) v2 2.60 GHz (80 W)

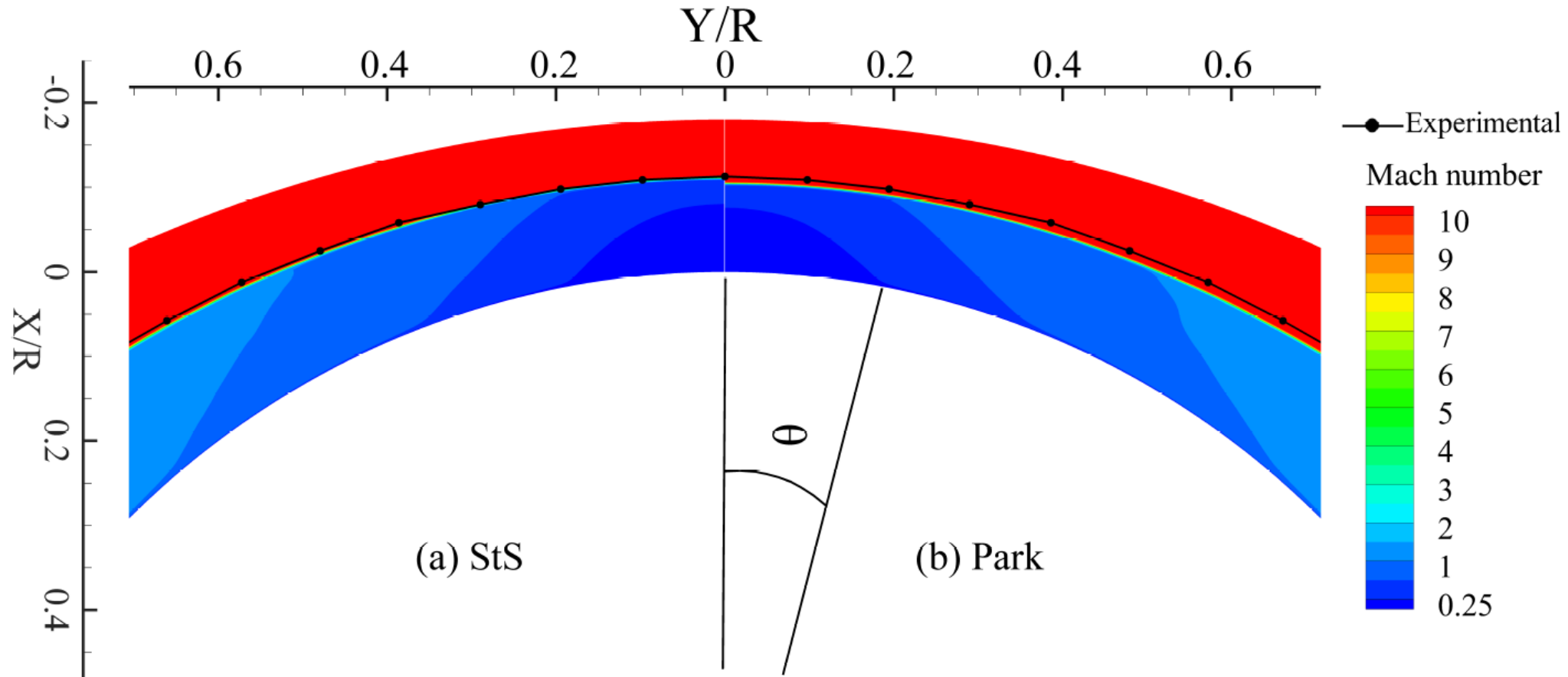
StS	Fluid cells	12 GPUs --Time per iteration (s) (Energy (J))	12 CPUs -- Time per iteration (s) (Energy(J))	Speed up (1 GPU vs 1 core)
	64x32	6.33 ($1.8 \cdot 10^4$)	8.17 ($7.8 \cdot 10^3$)	1.29 (7.7)
	128x64	6.36 ($1.8 \cdot 10^4$)	26.71 ($2.56 \cdot 10^4$)	4.2 (25.2)
	256x128	6.90 ($1.9 \cdot 10^4$)	105.9 ($10.2 \cdot 10^4$)	15.3 (91.8)
	512x256	15.91 ($4.5 \cdot 10^4$)	419.5 ($40.3 \cdot 10^4$)	26.4 (158.4)
	1024x512	68.72 ($19.4 \cdot 10^4$)	1702.1 ($163.4 \cdot 10^4$)	24.8 (148.8)

Park

64x32	$7.50 \cdot 10^{-3}$ (21)	$1.59 \cdot 10^{-3}$ (1.5)	0.21 (1.3)
128x64	$7.77 \cdot 10^{-3}$ (22)	$4.55 \cdot 10^{-3}$ (4.3)	0.59 (3.5)
256x128	$7.24 \cdot 10^{-3}$ (20)	$1.68 \cdot 10^{-2}$ (16)	2.32 (13.9)
512x256	$1.36 \cdot 10^{-2}$ (38)	$6.53 \cdot 10^{-2}$ (63)	4.8 (28.8)
1024x512	$3.48 \cdot 10^{-2}$ (98)	$2.46 \cdot 10^{-1}$ (236)	7.1 (42.6)

Flow past a sphere: Nonaka⁴ test case

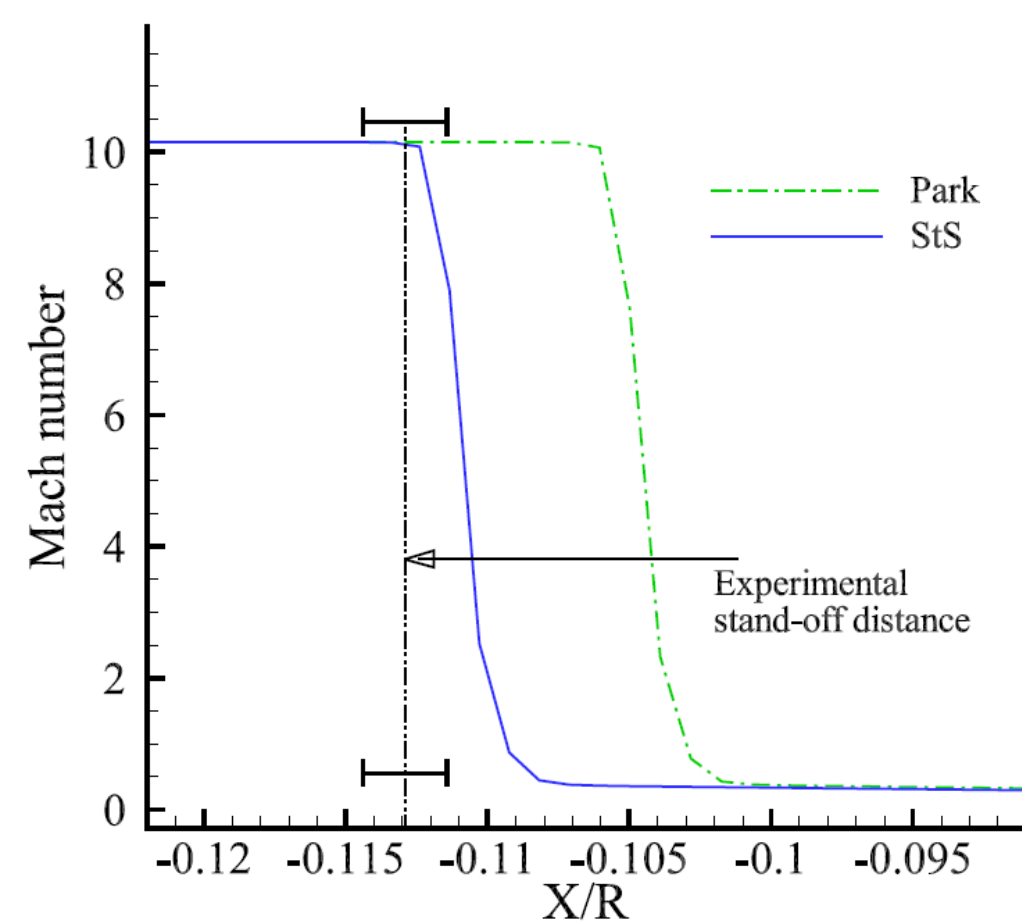
⁴ $R = 7\text{mm}$; $u_\infty = 3490\text{ m/s}$; $T_\infty = 293\text{ K}$; $P_\infty = 4825\text{ Pa}$; $Y_{\text{N}_2} = 0.767$; $Y_{\text{O}_2} = 0.233$



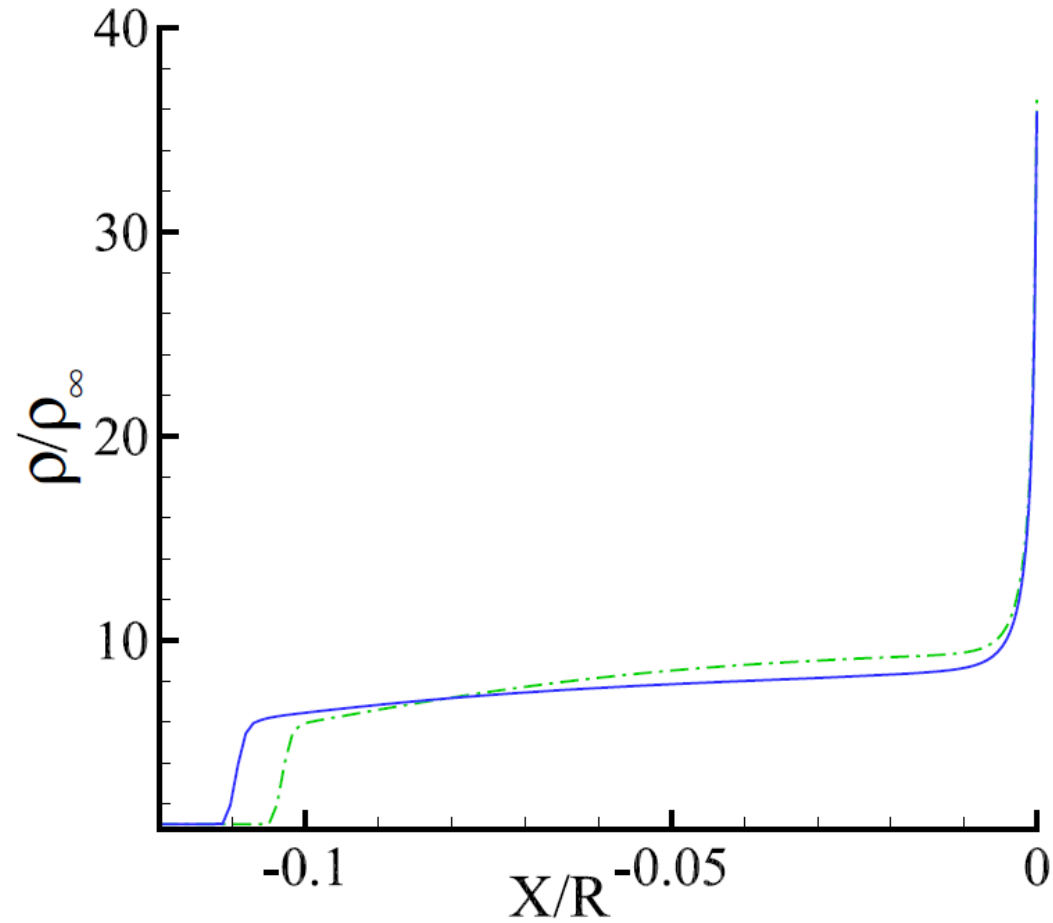
Numerical and experimental shock shape: (a) StS model; (b) Park model

⁴S. Nonaka et al. ,JTHT 14 (2), 2000

Nonaka⁴ test case: stagnation line profiles

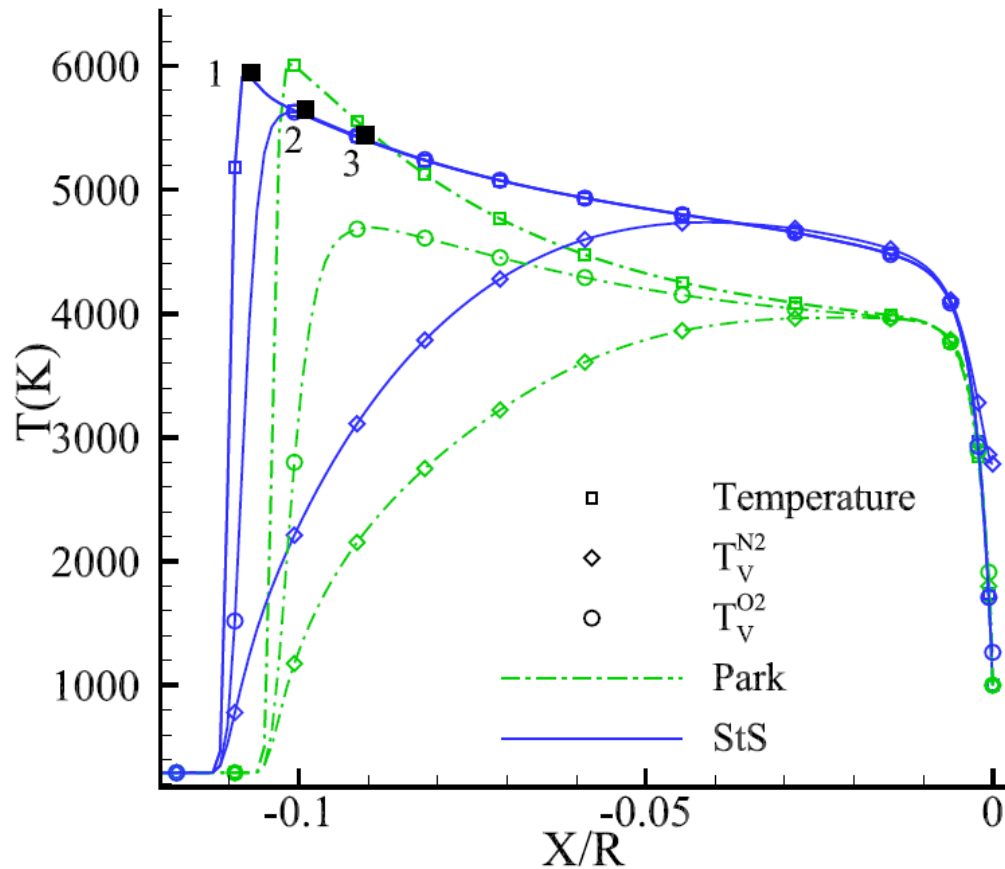


Mach Number

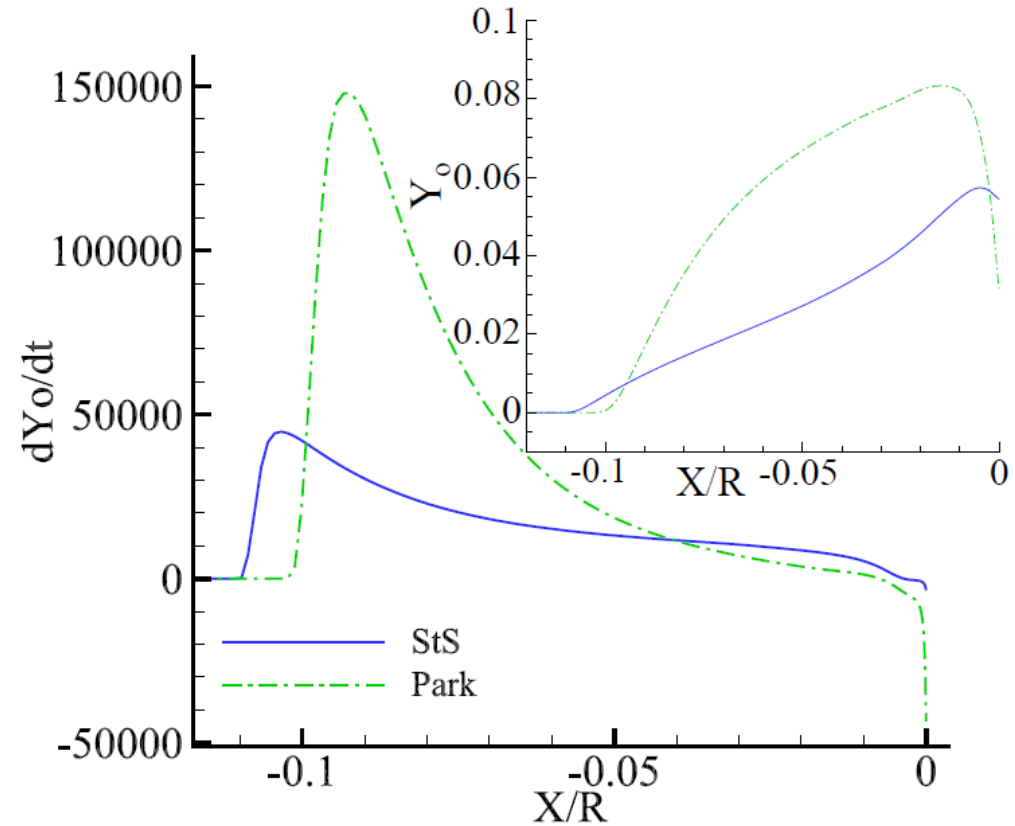


Normalized density

Nonaka⁴ test case: stagnation line profiles

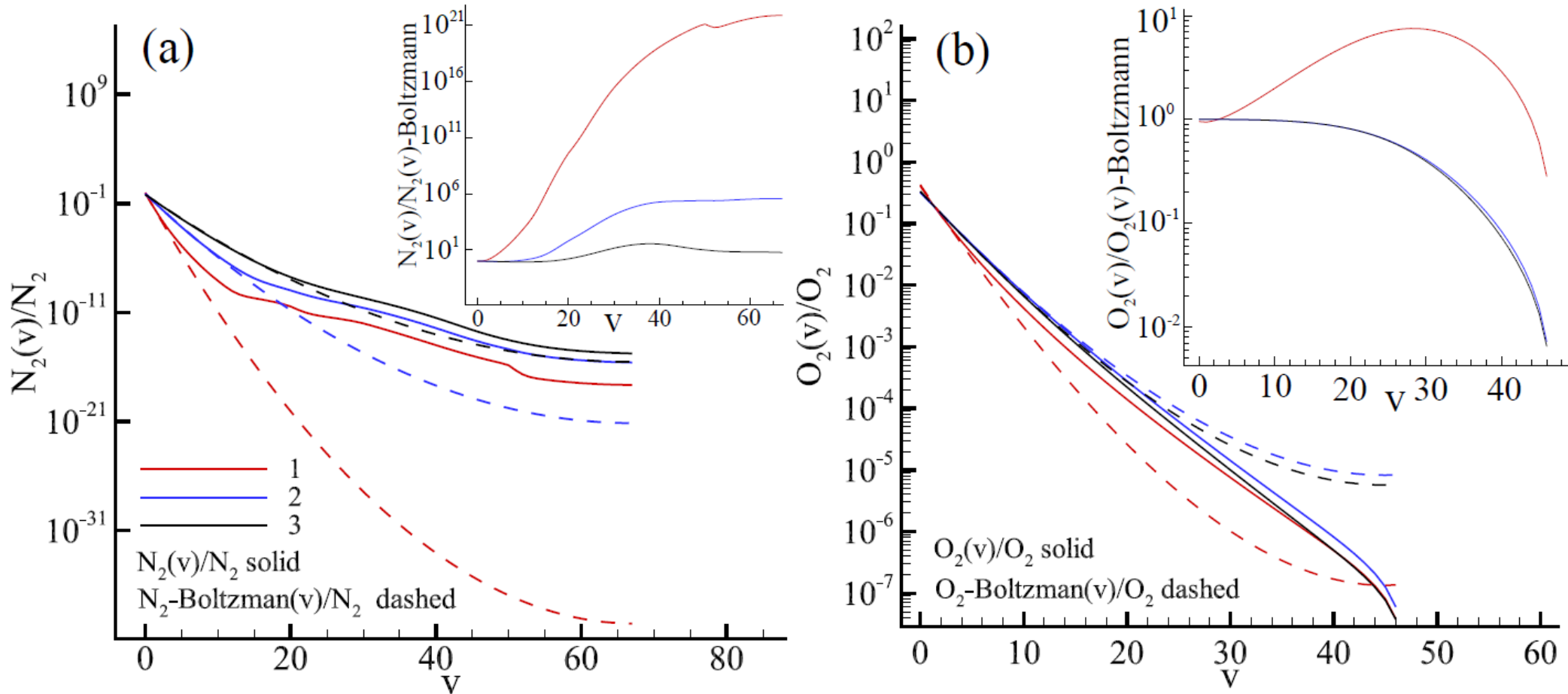


Temperatures



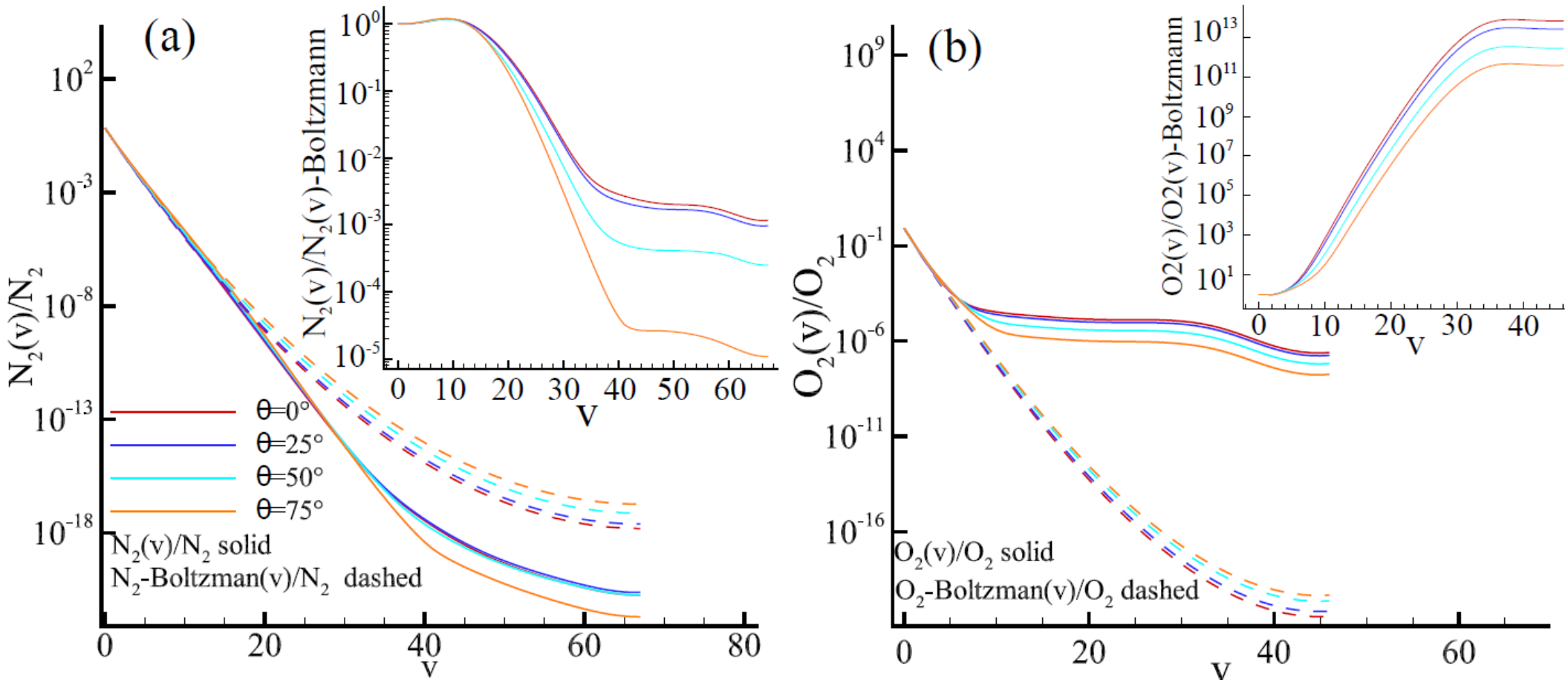
Oxygen atom reaction rate and mass fraction

Nonaka⁴ test case: vibrational distributions along stagnation line



Stagnation line population with actual to Boltzmann ratio in the inset: (a) N_2 ; (b) O_2

Nonaka⁴ test case: vibrational distributions wall profiles



Wall surface populations with actual to Boltzmann ratio in the inset: (a) N₂; (b) O₂

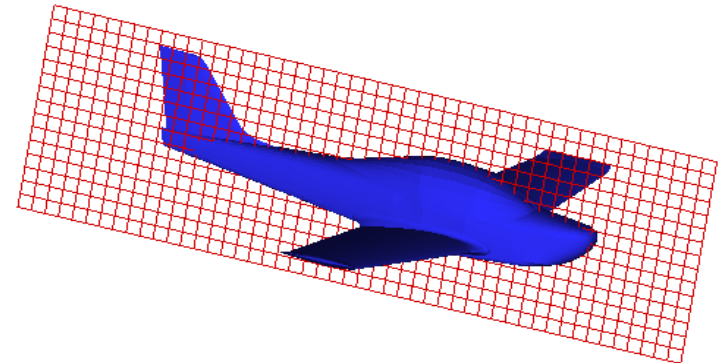
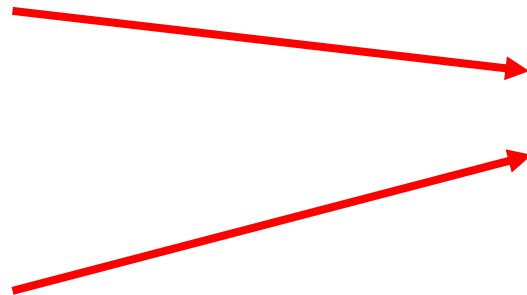
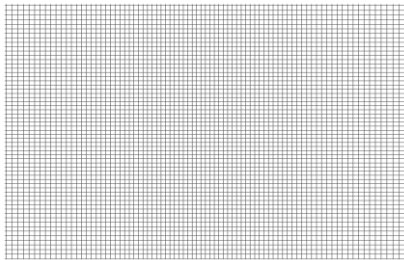
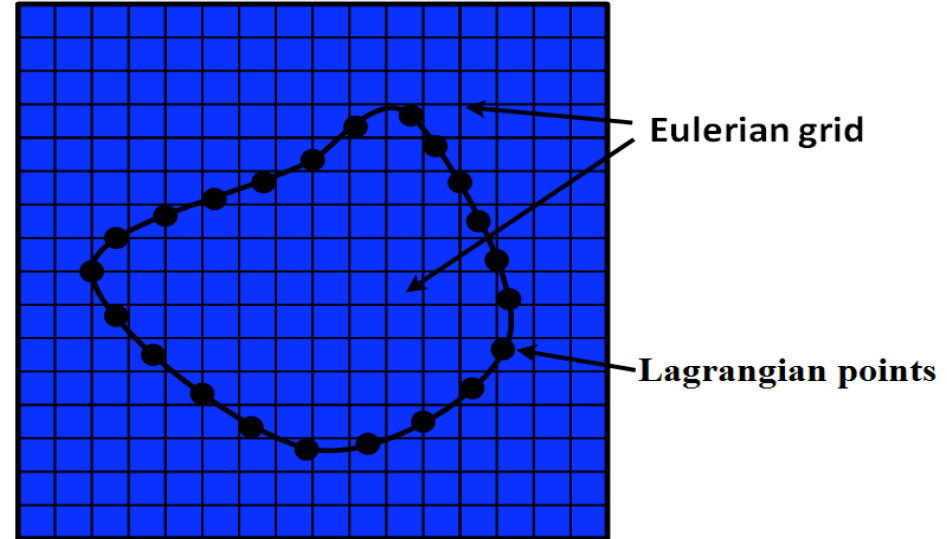
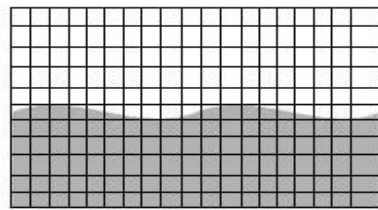
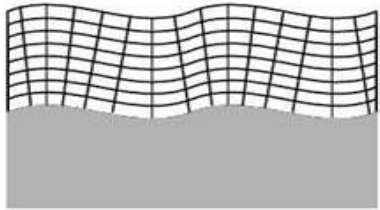
Immersed-Boundary Method

Geometry

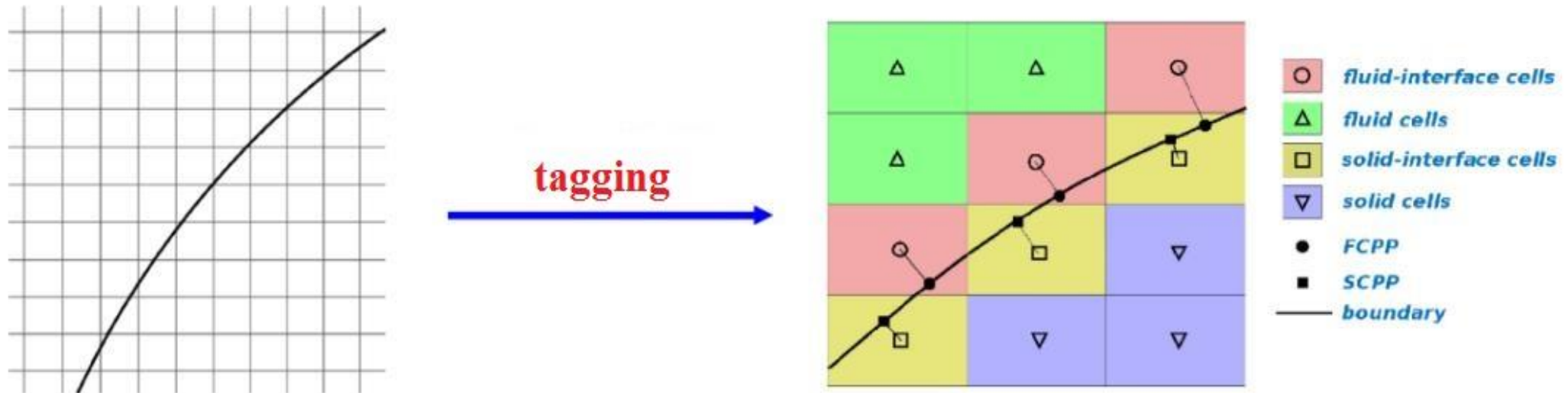
Cope with the time consuming grid generation and remeshing processes

Body-fitted mesh

IB method



Immersed-Boundary solver for Cartesian grid



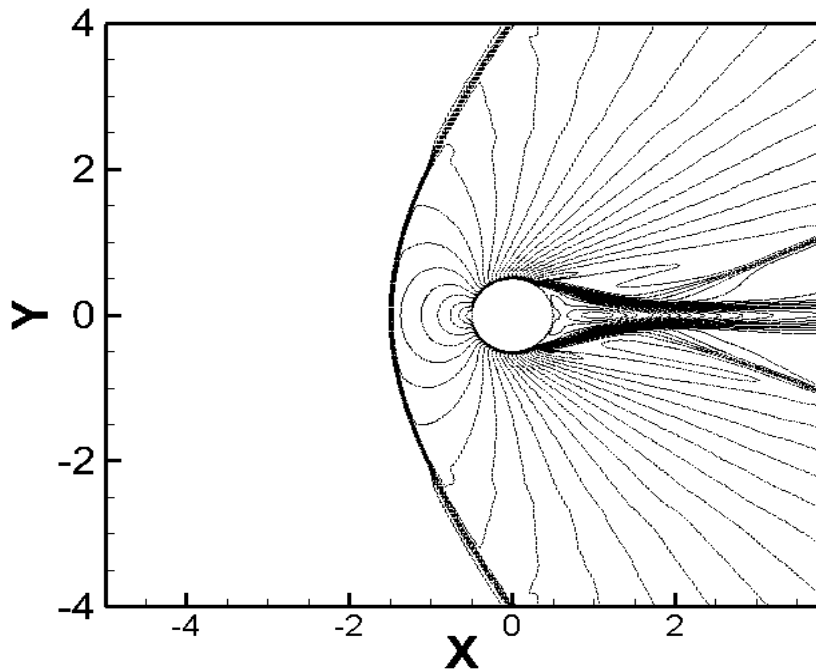
- the centers of the *fluid-interface* and *solid-interface* cells are projected onto the body surface along its normal direction, so as to obtain *fluid-cell projection points (FCPP)* and *solid-cell projection points (SCPP)*;
- the flow variables at the centers of the *fluid* cells and the temperature at the *solid* cells are the unknowns to be computed using a finite-volume dual time stepping solver;
- the *solid* cells do not influence the flow field at all and vice versa;
- the boundary conditions are imposed at the *fluid-interface* and *solid-interface* cells by a local IB reconstruction scheme.

Supersonic flow past a circular cylinder

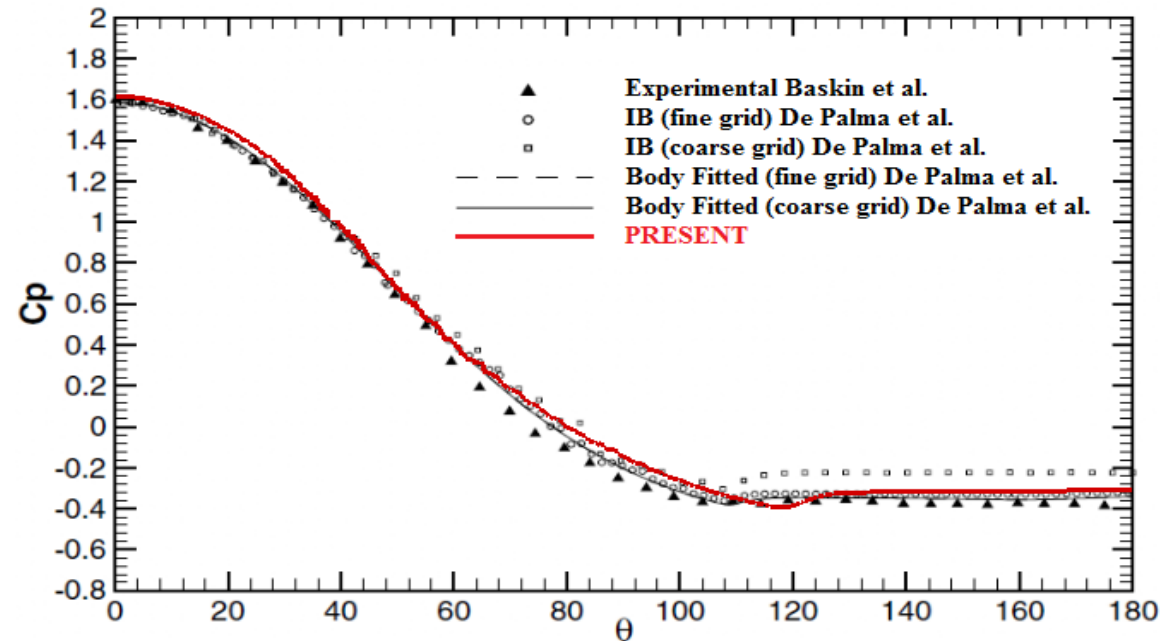
The new LS reconstruction has been validated and compared with the 1D reconstruction in the case of supersonic turbulent flow past a circular cylinder.

Re = 2000000, Ma = 1.7.

Grid: 139777 cells



Mach number contours on the finest grid, $\Delta Ma = 0.03$.



Pressure coefficient distributions along the external surface of the cylinder.

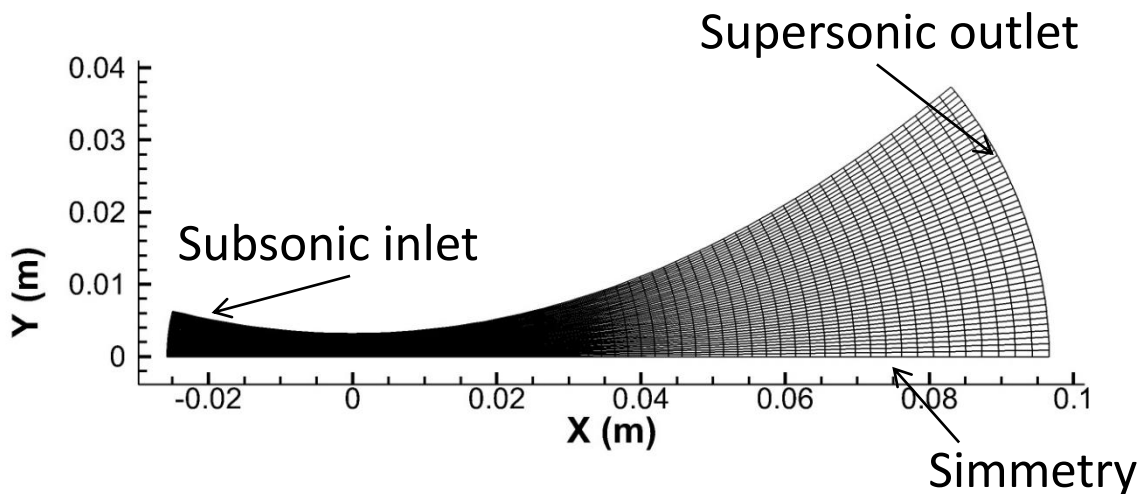
[1] De Palma et al., *Computers & Fluids*, 2006

[2] Bashkin et al., *Fluid Dynamics*, 2002

Sharma nozzle test case

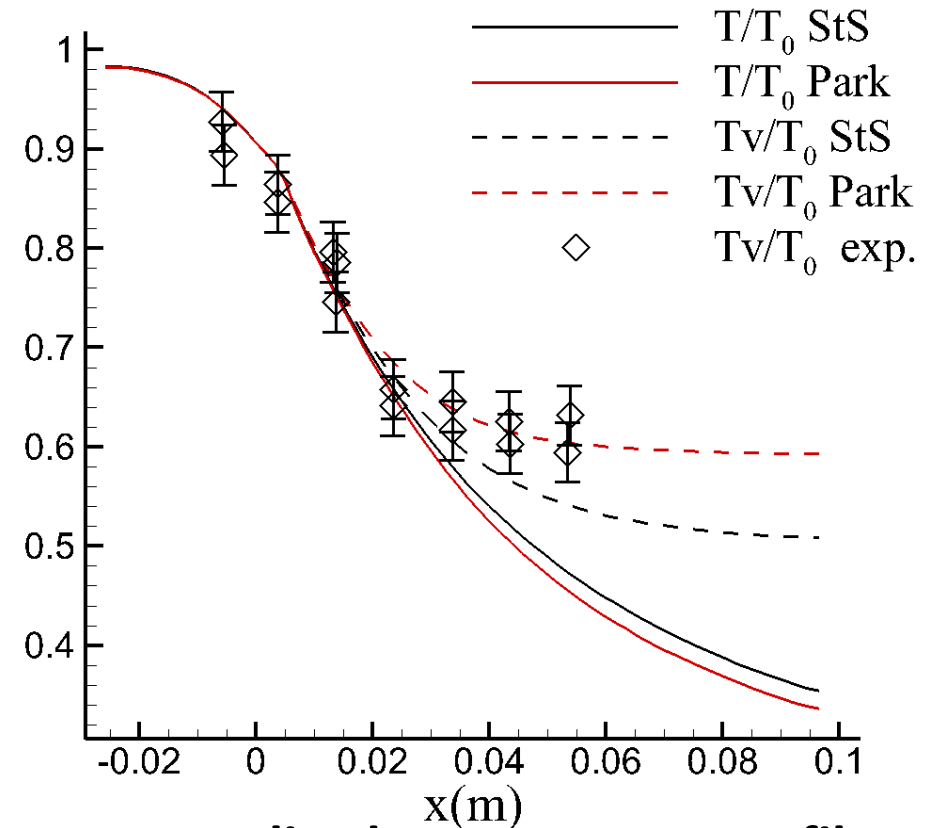
	Before throat	After throat
P	$P_0 = 100$ atm	0.197 atm
T	$T_0 = 5600$ K	300 K
(u, v)	(0, 0)	(0, 0)
N_2 molar fraction ^a	0.9828	1
$N_2(v)$ distribution	Boltzmann at T_0	Boltzmann at 300 K
N molar fraction ^a	0.0172	1.12923e-79

^aEquilibrium calculation.



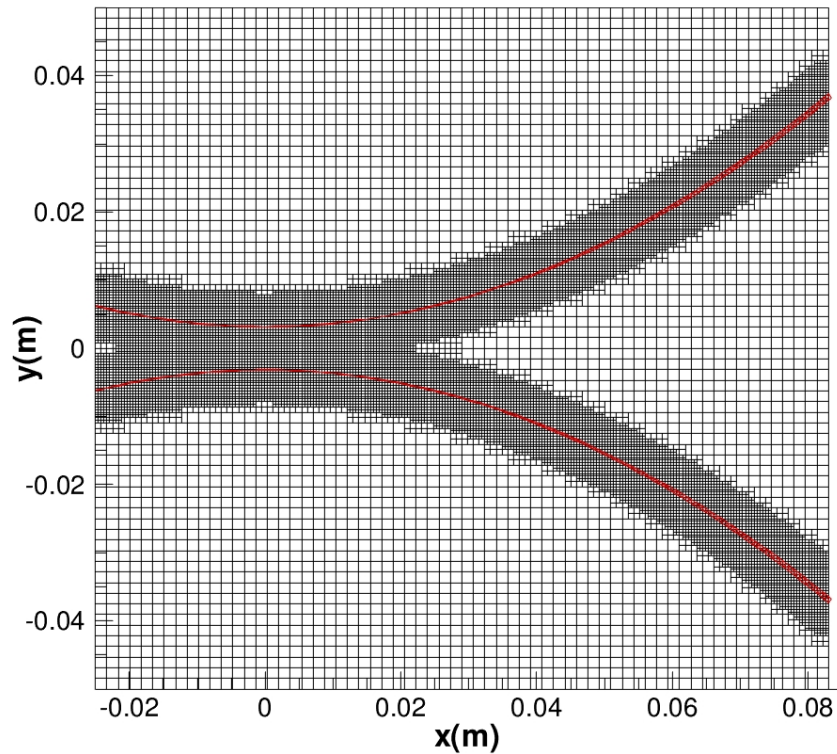
Grid scheme: 65x47 fluid cells

Initial conditions



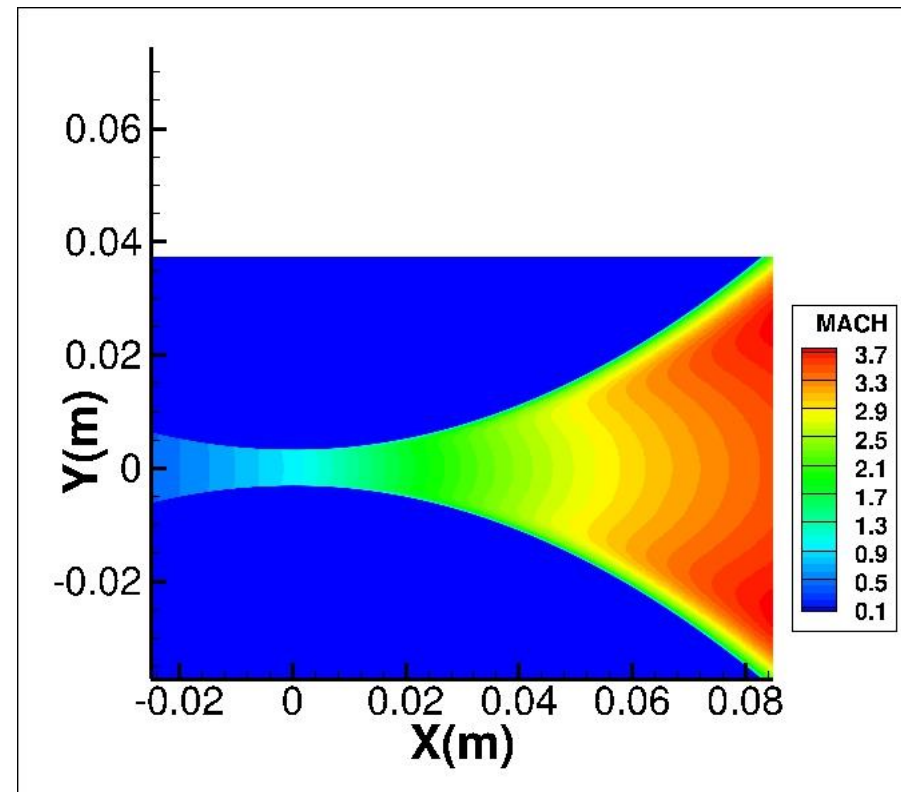
Normalized temperature profiles

Immersed-Boundary Method: Sharma nozzle test case

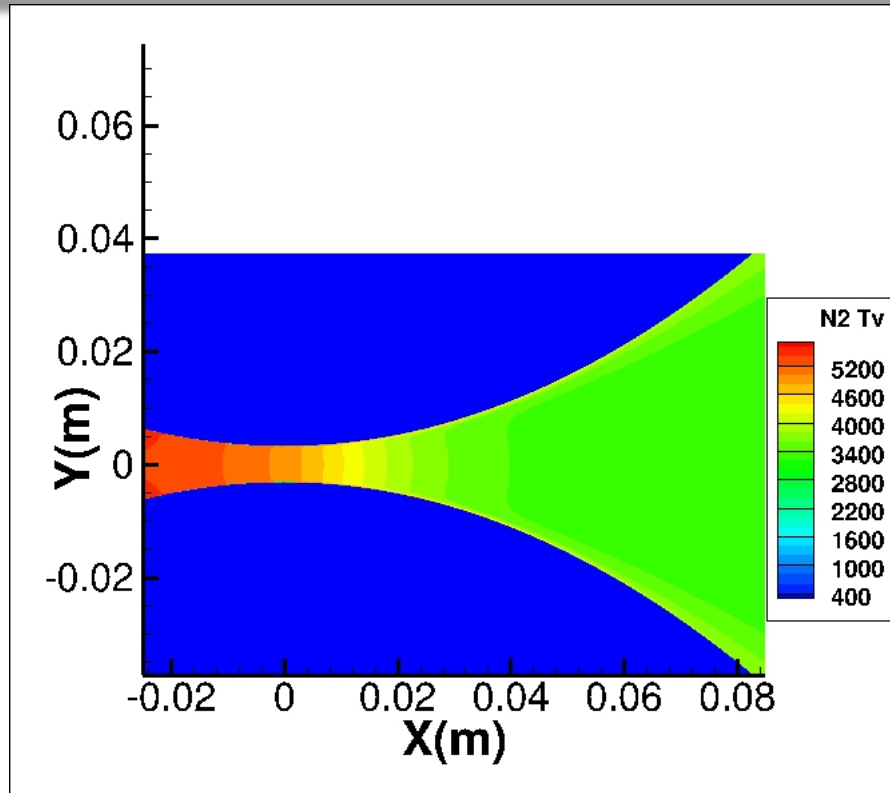


Cartesian mesh

Mach number contours

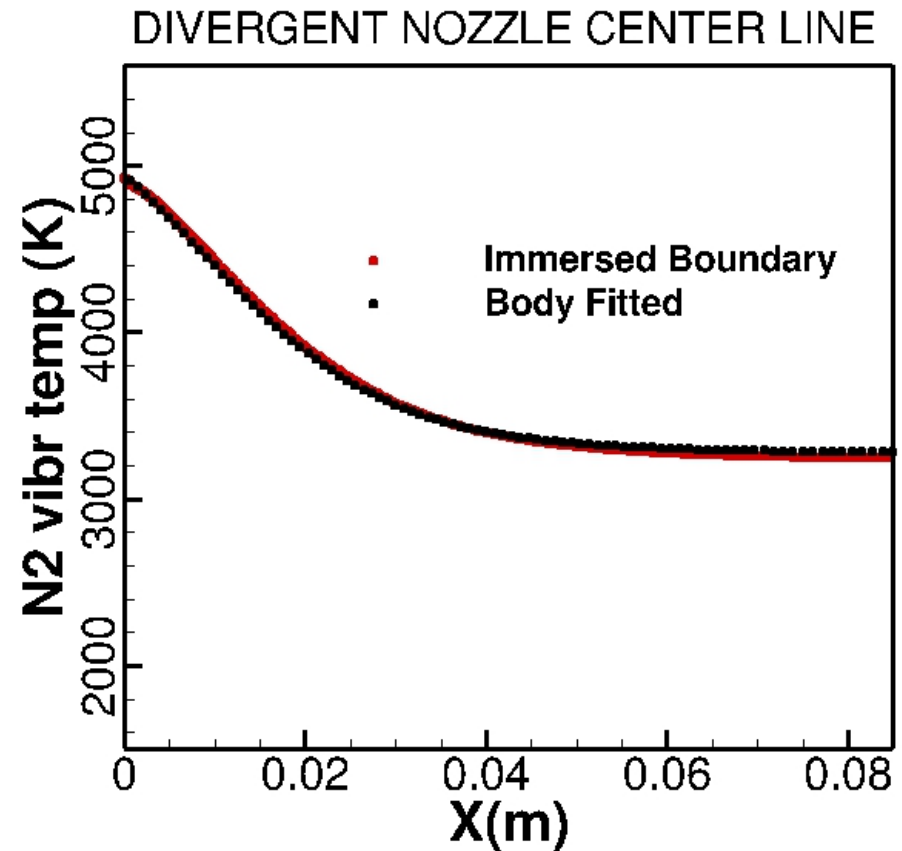


Immersed-Boundary Method: Sharma nozzle test case

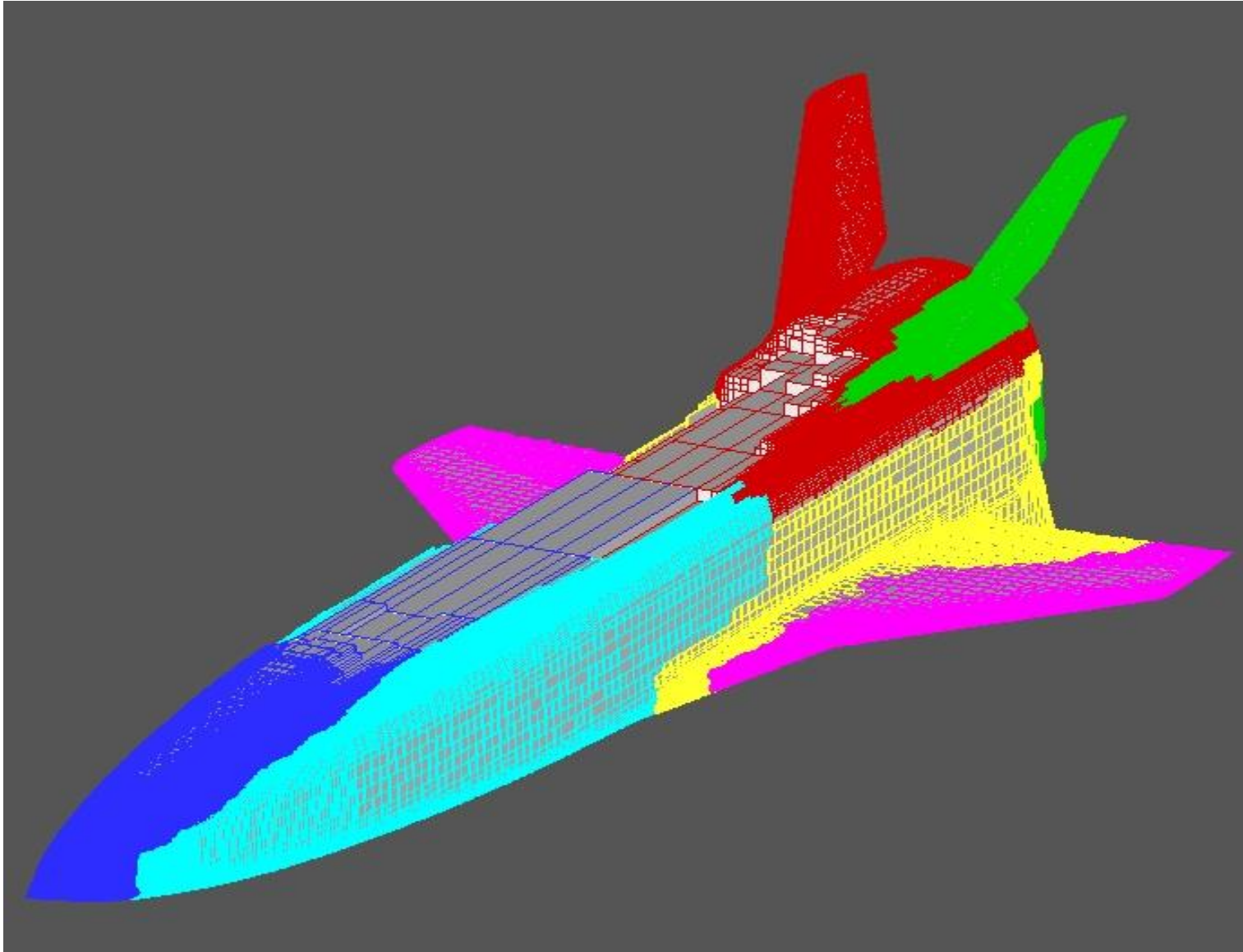


N2 T_v contours

IB vs Body fitted

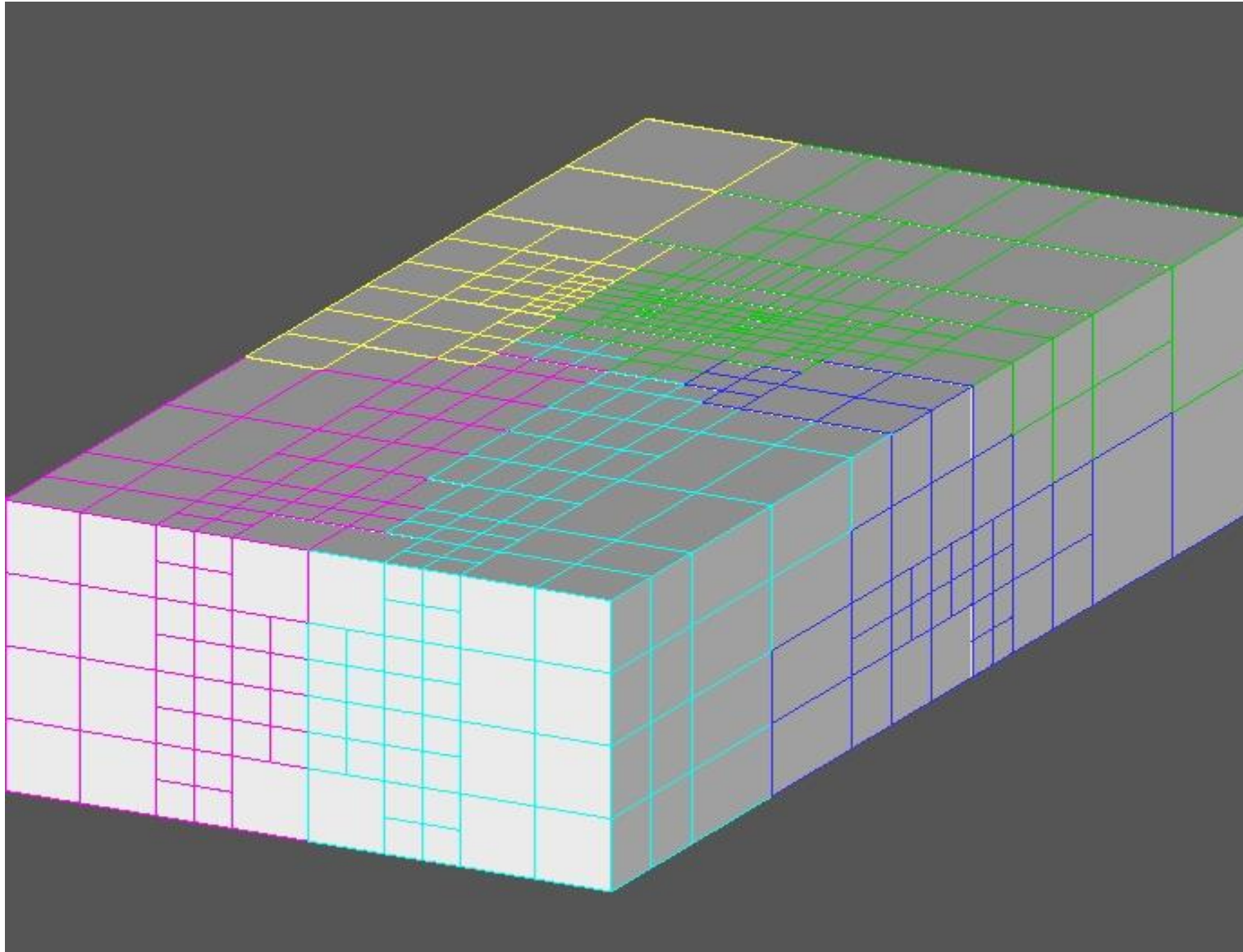


Computational mesh: internal points (solid)



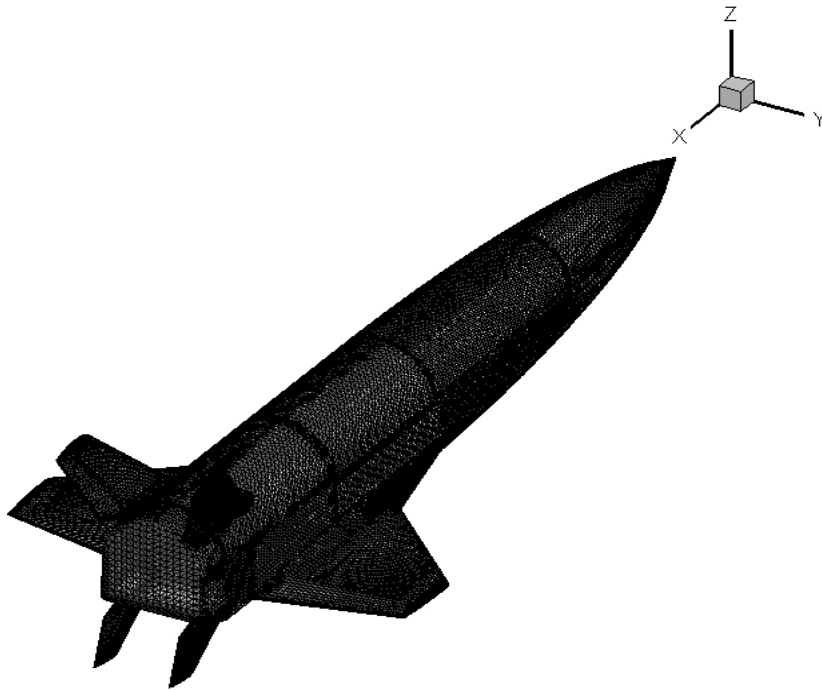
USV – Unmanned Space Vehicle

Computational mesh: external points (fluid)

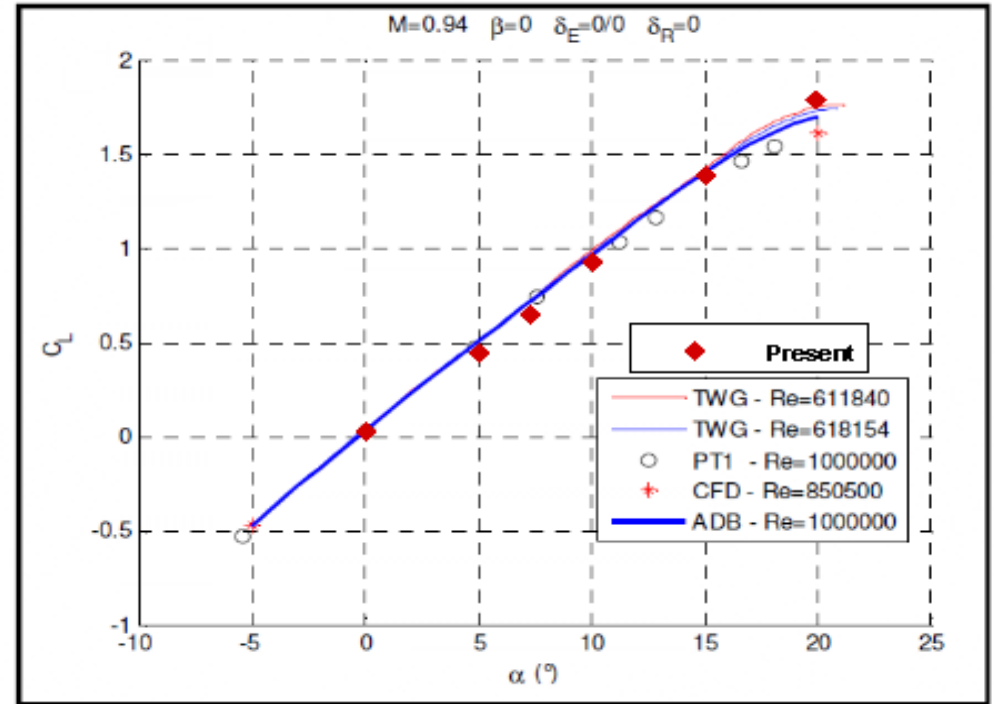


USV – Unmanned Space Vehicle

Transonic flow past an Unmanned Space Vehicle



Triangular mesh of the Unmanned Space Vehicle



C_L vs α at $M = 0.94$

α is the angle of attack

β is the side-slip angle

δ_E is the elevon deflection angle

δ_R is the rudder deflection angle

Conclusions

- We developed an efficient multi-GPU code for two-dimensional fluid dynamics
- We demonstrated the accuracy and the feasibility of fluid dynamic computations of thermochemical non-equilibrium flows by means of detailed state-to-state (StS) vibrationally resolved air kinetics
- The MPI-CUDA approach allowed us to efficiently scale the code across a multiple-nodes GPU cluster with good scalability performance: comparing the single GPU against the single core CPU performance speed-up values up to 150 were found.

Current and **future** work

- Flow-wall boundary treatment: models for catalysis and ablation
- Extension to 3D with a high-resolution hybrid WENO/central difference scheme
- **Introduction of ionized species**



Associazione Italiana Di Aeronautica e Astronautica

Web site <https://www.aidaa.it/>

The 2019 AIDAA Congress

The biennial Congress of the Italian
Association of Aeronautics and Astronautics



2019 **AIDAA**→
XXV INTERNATIONAL CONGRESS

September 9-12, 2019 @ University of Rome "Sapienza"

Associazione Italiana Di Aeronautica e Astronautica

Web site <https://www.aidaa.it/>



Aerotecnic Missili & Spazio

Since 1920 Official Journal of AIDAA
Now published with **Springer**

<https://www.springer.com/engineering/mechanical+engineering/journal/42496>